Inorg. Chem. **2008**, *47*, 5122–5128

Inorganic Chemistry

Article

Reversible Anion Exchange and Sensing in Large Porous Materials Built from 4,4′-Bipyridine via $\pi\cdots\pi$ and H-Bonding Interactions

Yongcai Qiu,[†] Zhihui Liu,[†] Yinghua Li,[†] Hong Deng,[*,†] Ronghua Zeng,[†] and Matthias Zeller[*,‡]

School of Chemistry and Environment, South China Normal University, Guangzhou, 510006, P.R. China, and Department of Chemistry, Youngstown State University, One University Plaza, Youngstown, Ohio 44555-3663

Received December 5, 2007

Two unusual d^{10} compounds, $[Zn_2(bipy)_3(H_2O)_8(ClO_4)_2(paba)_2]\cdot 2(bipy)\cdot 4H_2O$ (**1**) and $[Cd_2(bipy)_4(H_2O)_6(ClO_4)_2(paba)_2]\cdot(bipy)\cdot 5H_2O$ (**2**) (bipy = 4,4′-bipyridine, paba = *p*-aminobenzoate), were obtained from reaction of the metal salts, bipy and paba in an EtOH/H_2O mixture. The bipy ligands in the two compounds exhibit two new modes of coordinating to transition metal ions, resulting in the formation of large porous frameworks. Immersion of single crystals of **1** in an aqueous solution of NH_4PF_6 results in the formation of its hexafluorophosphate derivative **3** as shown by single crystal diffraction. Immersion of crystals of **3** in $NaClO_4$ regenerates **1**. Furthermore, compound **1** also shows interesting anion sensing properties in an EtOH/H_2O mixture.

Introduction

The design and construction of open framework supramolecular coordination materials have attracted great attention in recent years owing to their interesting topologies, their potential applications in catalysis, gas storage, and molecular recognition, and their magnetic, electrical, and nonlinear optical properties.[1–4] Porous materials such as Prussian Blue,[5] certain Werner complexes,[6] and Hofmann clathrates and their derivatives[7] are well-known to reversibly absorb small molecules, and numerous examples of porous organic frameworks were constructed via hydrogen bonding, $\pi\cdots\pi$ contacts, and other less than covalent interactions.[8] In the vast amount of the reported work, a variety of 1D, 2D, and 3D molecular open frameworks have been successfully obtained via the use of coordinating functional groups, such as carboxylates, bipy or its derivatives, and mixtures of both carboxylate and bipy ligands.[9,10] There are also a tremendous number of porous coordination polymers with cavities that accommodate bipy or its derivatives but only very few examples have yet been reported to enclathrate mixtures of aromatic carboxylates and bipy ligands as large organic guest

---

[*] To whom correspondence should be addressed. E-mail: dh@scnu.edu.cn (H.D.), mzeller@cc.ysu.edu (M.Z.).

[†] South China Normal University.

[‡] Youngstown State University.

(1) (a) Review articles Stang, P. J.; Olenyuk, B. *Acc. Chem. Res.* **1997**, *30*, 502. (b) Batten, S.; Robson, R. *Angew. Chem., Int. Ed.* **1998**, *37*, 1460. (c) Cheetham, A. K.; Ferey, G.; Loiseau, T. *Angew. Chem., Int. Ed.* **1999**, *38*, 3268. (d) Janiak, C. *Dalton Trans.* **2003**, 2781. (e) Bradshaw, D.; Claridge, J. B.; Cussen, E. J.; Prior, T. J.; Rosseinsky, M. J. *Acc. Chem. Res.* **2005**, *38*, 273. (f) Ferey, G.; Mellot-Draznieks, C.; Serre, C.; Millange, F. *Acc. Chem. Res.* **2005**, *38*, 217.

(2) (a) Yaghi, O. M.; Li, G. *Nature* **1995**, *378*, 703. (b) Li, H.; Eddaoudi, M.; O'Keeffe, M.; Yaghi, O. M. *Nature* **1999**, *402*, 276. (c) Seo, J. S.; Whang, D.; Lee, H.; Jun, S. I.; Oh, J.; Jeon, Y. J.; Kim, K. *Nature* **2000**, *404*, 982. (d) Eddaoudi, M.; Kim, J.; Rosi, N.; Vodak, D.; Wachter, J.; O'Keeffe, M.; Yaghi, O. M. *Science* **2002**, *295*, 469. (e) Muller, A. *Science* **2003**, *300*, 749.

(3) (a) Rao, C. N. R.; Natarajan, S.; Vaidhyanathan, R. *Angew. Chem., Int. Ed.* **2004**, *43*, 1466. (b) Ding, B.-B.; Weng, Y.-Q.; Mao, Z.-W.; Lam, C.-K.; Chen, X.-M.; Ye, B.-H. *Inorg. Chem.* **2005**, *44*, 8836. (c) Pan, L.; Olson, D. H.; Ciemnolonski, L. R.; Heddy, R.; Li, J. *Angew. Chem., Int. Ed.* **2006**, *45*, 616. (d) Fang, Q.; Zhu, G.; Xue, M.; Sun, J.; Sun, F.; Qiu, S. *Inorg. Chem.* **2006**, *45*, 3582.

(4) (a) Markus, A. *Angew. Chem., Int. Ed.* **1999**, *38*, 3463. (b) Abrahams, B. F.; Batten, S. R.; Grannas, M. J.; Hamit, H.; Hoskins, B. F.; Robson, R. *Angew. Chem., Int. Ed.* **1999**, *38*, 1475. (c) Seidel, S. R.; Stang, P. J. *Acc. Chem. Res.* **2002**, *35*, 972. (d) Kumazawa, K.; Biradha, K.; Kusukawa, T.; Okano, T.; Fujita, M. *Angew. Chem., Int. Ed.* **2003**, *42*, 3909. (e) Behrens, E. A.; Poojary, D. M.; Clearfield, A. *Chem. Mater.* **1996**, *8*, 1236. (f) Becht, G.; Hwu, S.-J. *Chem. Mater.* **2006**, *18*, 4221.

(5) (a) Barrer, R. M. In *Molecular Sieves*; Meier, W. M., Utyyerhoeven, J. B., Eds.; ACS Advances in Chemistry Series 121; American Chemical Society: Washington, DC, 1974; p 1.

(6) (a) Buser, H. J.; Schwarzenbach, D.; Petter, W.; Ludi, A. *Inorg. Chem.* **1977**, *16*, 2704. (b) Dunbar, K. R.; Heintz, R. A. *Prog. Inorg. Chem.* **1997**, *45*, 283.

(7) Iwamoto, T. In *Inclusion Compounds*; Atwood, J. L., Davies, J. E. D., MacNicol, D. D., Eds.; Oxford: New York, 1991; Vol. *5*, p 177.

(8) (a) Dewa, T.; Endo, K.; Aoyama, Y. *J. Am. Chem. Soc.* **1998**, *120*, 8933. (b) Braga, D.; Desiraju, G. R.; Miller, J. S.; Orpen, A. G.; Orpen, A. G.; Price, S. L. *CrystEngComm.* **2002**, *4*, 500. (c) Biradha, K. *CrystEngComm.* **2003**, *5*, 374. (d) Braga, D. *Chem. Commun.* **2003**, 2751. (e) Moulton, B.; Zaworotko, M. J. *Chem. Rev.* **2001**, *101*, 1629. (f) Kitagawa, S.; Kitaura, R.; Noro, S. *Angew. Chem., Int. Ed.* **2004**, *43*, 2334.

10.1021/ic702366t CCC: $40.75

© 2008 American Chemical Society
Published on Web 05/10/2008

molecules.[11] Although *p*-aminobenzoic acid and 4,4′-bipy ligands had been chosen to construct coordination compounds by Chen and Hong,[12] they did not isolate compounds that enclathrate all primary ligands (bipy and *p*-paba).

Ions and small molecules, when being incorporated as guest species in coordination compounds, do not only have a major influence on the construction of the networks and may lead to novel geometries,[13] but the new host–guest materials may also play an important role in materials science, for example, in roles such as chemical sensors and ion exchange materials.[14–16] Kitagawa et al., for example, successfully constructed a series of porous Cu(II)/4,4′-bipy coordination polymers via addition of different anions.[17] In coordination networks in general the 4,4′-bipy ligands may act in bidentate bridging or monodentate terminal modes, resulting in 1D linear, zigzag, ladder, molecular antenna railroads and chains, 2D bilayer, square and rectangular grid networks, or 3D noninterpenetrated and interpenetrated networks.

On the basis of these studies, we hoped to obtain compounds similar to the above-mentioned with large cavities and noninterpenetrating character. The selection of the anionic and organic ionic components is crucial for the construction of compounds with intriguing structural motifs and potentially useful properties.[13–17] To achieve this goal, we chose *p*-aminobenzoic acid as a good N- and O-donor, as well as O-acceptor, and rod-like rigid 4,4′-bipy as the bridging ligand of choice. We have been able to isolate two unusual d^{10} compounds, namely, $[Zn_2(bipy)_3(H_2O)_8(ClO_4)_2(paba)_2]\cdot 2(bipy)\cdot 4H_2O$ (**1**) and $[Cd_2(bipy)_4(H_2O)_6(ClO_4)_2(paba)_2]\cdot(bipy)\cdot 5H_2O$ (**2**). The 4,4′-bipy ligands in the two compounds exhibit two new coordination modes to transition metal ions, resulting in the formation of large porous frameworks hosting the organic ligands, anions, and water molecules via weak noncovalent bonding interactions.

Experimental Section

General Remarks. All the materials and reagents were obtained commercially and used without further purification. Elemental (C, H, N) analyses were performed on a Perkin-Elmer 2400 element analyzer. Infrared (IR) samples were prepared as KBr pellets, and spectra were obtained in the 4000–400 cm^{-1} range using a Nicolet Avatar 360 FT-IR spectrophotometer. Fluorescence spectra were recorded with an Edinburgh F900 FL Spectrophotometer analyzer. The pore volume analysis was accomplished using the Platon software.[18]

Preparation of Compound 1. A mixture of $Zn(NO_3)_2\cdot 6H_2O$ (0.297 g; 1 mmol), 4,4′-bipy (0.156 g; 1 mmol), and 75% ethanol 20 mL solution was stirred for 30 min at 70 °C, then added to *p*-aminobenzoic acid (0.5 mmol), and adjusted to pH 7.0 with an aqueous solution of sodium hydroxide (0.1 mol/L). The mixture was continuously stirred for another 30 min and filtered. Then, three drops of saturated $NaClO_4$ solution were added to the filtrate. Colorless blocky single crystals were obtained at room temperature by slow evaporation of the filtrate after several days. Anal. Calcd for $C_{64}H_{76}Zn_2N_{12}O_{24}Cl_2$ (%): C, 48.07; H, 4.79; N, 10.51. Found: C, 47.95; H, 4.86; N, 10.60. IR frequencies (KBr, cm^{-1}): 3375, 1627, 1597, 1543, 1489, 1429, 1367, 1330, 1203, 1165, 1097, 1058, 1008, 813, 702.

Preparation of Compound 2. The same synthetic procedure as for compound **1** was employed except that $Zn(NO_3)_2\cdot 6H_2O$ was replaced by $Cd(NO_3)_2\cdot 4H_2O$ (0.308 g; 1 mmol), resulting in colorless blocky single crystals. Anal. Calcd for $C_{64}H_{74}Cd_2Cl_2N_{12}O_{23}$ (%): C, 45.89; H, 4.45; N, 10.03. Found: C, 45.75; H, 4.43; N, 10.09. IR frequencies (KBr, cm^{-1}): 3441, 1624, 1604, 1531, 1489, 1411, 1379, 1311, 1219, 1196, 1116, 1089, 1043, 1006, 800, 705.

Preparation of Compound 3. Single crystals of **1** were immersed in an aqueous NH_4PF_6 solution (0.2 mmol) over one week to obtain single crystals of **3**. Anal. Calcd for $C_{64}H_{76}Zn_2F_{12}N_{12}O_{16}P_2$ (%): C, 45.48; H, 4.53; N, 9.95. Found: C, 45.50; H, 4.56; N, 10.01. IR frequencies (KBr, cm^{-1}): 3380, 1628, 1598, 1541, 1489, 1428, 1365, 1334, 1201, 1054, 1006, 850, 812, 702, 569.

Preparation of Compound 4. Single crystals of **3** were reimmersed in an aqueous $NaClO_4$ solution (0.2 mmol) over one week to obtain single crystals of **4** (viz. **1**). Anal. Calcd for

---

(9) (a) Tong, M. L.; Chen, X. M. *CrystEngComm.* **2000**, 1. (b) Tong, M. L.; Chen, H. J.; Chen, X. M. *Inorg. Chem.* **2000**, *39*, 2235. (c) Li, X. J.; Rong, C.; Feng, D. F.; Bi, W. H.; Wang, Y.; Li, X.; Hong, M. C. *Cryst. Growth Des.* **2004**, *4*, 775. (d) Dai, J. C.; Wu, X.-T.; Hu, S.-M.; Fu, Z.-Y.; Zhang, J.-J.; Du, W.-X.; Zhang, H.-H.; Sun, R.-Q. *Eur. J. Inorg. Chem.* **2004**, 2096. (e) Qin, C.; Wang, X. L.; Carlucci, L.; Tong, M. L.; Wang, E. B.; Hu, C. W.; Xu, L. *Chem. Commun.* **2004**, 1876.

(10) (a) Liu, Q.-Y.; Xu, L. *CrystEngComm.* **2005**, *7*, 87. (b) Liao, Y.-C.; Liao, F.-L.; Chang, W.-K.; Wang, S.-L. *J. Am. Chem. Soc.* **2004**, *126*, 1320. (c) Fu, Z. Y.; Wu, X.-T.; Dai, J. C.; Hu, S.-M.; Du, W.-X. *New J. Chem.* **2002**, *26*, 978. (d) Prior, T. J.; Bradshaw, D.; Teat, S. J.; Rosseinsky, M. J. *Chem. Commun.* **2003**, 500.

(11) (a) Ayyappan, P.; Evans, O. R.; Li, W. *Inorg. Chem.* **2002**, *41*, 3328. (b) Fu, Z.-Y.; Wu, X.-T.; Dai, J.-C.; Hu, S.-M.; Du, W.-X. *New J. Chem.* **2002**, *26*, 978.

(12) (a) Sun, D. F.; Cao, R.; Sun, Y. Q.; Bi, W. H.; Li, X. J.; Wang, Y. Q.; Shi, Q.; Li, X. *Inorg. Chem.* **2003**, *42*, 7512. (b) Liu, C.-M.; Xiong, R.-G.; You, X.-Z.; Chen, W. *Acta Chem. Scand.* **1998**, *52*, 1353.

(13) (a) Tong, M.-L.; Zheng, S.-L.; Chen, X.-M. *Polyhedron.* **2000**, *19*, 1809. (c) Wang, R.; Hong, M.; Luo, J.; Jiang, F.; Han, L.; Lin, Z.; Cao, R. *Inorg. Chim. Acta* **2004**, *357*, 103. (d) Wang, R.; Jiang, F.; Zhou, Y.; Han, L.; Hong, M. *Inorg. Chim. Acta* **2005**, *358*, 545. (e) Barnett, S. A.; Champness, N. R. *Coord. Chem. Rev.* **2003**, *246*, 145. (f) Biradha, K.; Sarkar, M.; Rajput, L. *Chem. Commun.* **2006**, 4169.

(14) (a) Yang, G.-D.; Dai, J.-C.; Lian, Y.-X.; Wu, W.-S.; Lin, J.-M.; Hu, S.-M.; Sheng, T.-L.; Fu, Z.-Y.; Wu, X.-T. *Inorg. Chem.* **2007**, *46*, 7910. (b) Ohmori, O.; Kawano, M.; Fujita, M. *J. Am. Chem. Soc.* **2004**, *126*, 16292. (c) Saied, O.; Maris, T.; Wuest, J. D. *J. Am. Chem. Soc.* **2003**, *125*, 14956. (d) Choi, H. J.; Suh, M. P. *J. Am. Chem. Soc.* **2004**, *126*, 15844. (e) Davis, A. V.; Fiedler, D.; Seeber, G.; Zahl, A.; Eldik, R.; Raymond, K. N. *J. Am. Chem. Soc.* **2006**, *128*, 1324. (f) Chen, B. L.; Yang, Y.; Zapata, F.; Lin, G.; Qian, G. D.; Lobkovsky, E. B. *Adv. Mater.* **2007**, *19*, 1693. (h) Yaghi, O. M.; Li, H.; Groy, T. L. *Inorg. Chem.* **1997**, *36*, 4292.

(15) (a) Rood, J. A.; Noll, B. C.; Henderson, K. W. *Inorg. Chem.* **2006**, *45*, 5521. (b) Amaya, T.; Rebek, J., Jr. *J. Am. Chem. Soc.* **2004**, *126*, 14149. (c) Suh, M. P.; Ko, J. W.; Choi, H. J. *J. Am. Chem. Soc.* **2002**, *124*, 10976. (d) Malek, N.; Maris, T.; Simard, M.; Wuest, J. D. *J. Am. Chem. Soc.* **2005**, *127*, 5910. (e) Jacobs, A.; Faleni, N.; Nassimbeni, L. R.; Taljaard, J. H. *Cryst. Growth Des.* **2007**, *7*, 1003. (f) Soldatov, D. V.; Grachev, E. V.; Ripmeester, J. A. *Cryst. Growth Des.* **2002**, *2*, 401. (g) Davis, A. V.; Raymond, K. N. *J. Am. Chem. Soc.* **2005**, *127*, 7912. (h) Sarkar, M.; Biradha, K. *Cryst. Growth Des.* **2006**, *6*, 1742.

(16) (a) Amendola, V.; Esteban-Gómez, D.; Fabbrizzi, L.; Licchelli, M. *Acc. Chem. Res.* **2006**, *39*, 343. (b) Boiocchi, M.; Del Boca, L.; Esteban-Gómez, D.; Fabbrizzi, L.; Licchelli, M.; Monzani, E. *J. Am. Chem. Soc.* **2004**, *126*, 16507. (c) Wong, K.-L.; Law, G.-L.; Yang, Y.-Y.; Wong, W.-T. *Adv. Mater.* **2006**, *18*, 1051. (d) Chen, C.-L.; Goforth, A. M.; Smith, M. D.; Su, C.-Y.; zur Loye, H. *Angew. Chem., Int. Ed.* **2005**, *44*, 2.

(17) Noro, S.-I.; Kitaura, R.; Kondo, M.; Kitagawa, S.; Ishii, T.; Matsuzaka, H.; Yamashita, M. *J. Am. Chem. Soc.* **2002**, *124*, 2568.

(18) Spek, A. L. *PLATON, A Multipurpose Crystallographic Tool* Utrecht University: The Netherlands, 2005.

Table 1. Some Crystal, Data Collection, and Structure Refinement Parameters

compound	1	2	3	4
empirical formula	$C_{128}H_{152}Cl_4N_{24}O_{48}Zn_4$	$C_{64}H_{74}Cd_2Cl_2N_{12}O_{23}$	$C_{64}H_{76}F_{12}N_{12}O_{16}P_2Zn_2$	$C_{128}H_{152}Cl_4N_{24}O_{48}Zn_4$
fw	3198.02	1675.07	1690.05	3198.02
cryst syst	monoclinic	triclinic	monoclinic	monoclinic
space group	$P2_1/c$	$P\bar{1}$	$P2_1/c$	$P2_1/c$
a (Å)	19.2491(4)	7.5721(7)	19.3688(10)	19.257(1)
b (Å)	7.0267(1)	15.4801(14)	7.1578(4)	7.0227(3)
c (Å)	30.7964(5)	16.0700(15)	31.1351(12)	30.7970(16)
α (deg)		72.184(2)		
β (deg)	120.237(1)	84.553(2)	120.680(2)	120.279(3)
γ (deg)		82.995(2)		
V (Å^3)	3598.7(1)	1776.6(3)	3712.3(3)	3596.7(3)
Z	1	1	2	1
D_C (g/cm^3)	1.476	1.566	1.512	1.476
μ mm^{-1}	0.827	0.759	0.792	0.827
F (000)	1660	856	1740	1660
parameters	506	601	487	506
goodness-of-fit	1.033	0.965	1.103	1.081
$R_1{}^a$	0.0476, 0.0888	0.0441, 0.0648	0.0597, 0.0898	0.0528, 0.1070
$wR_2{}^b$	0.1057,0.1245	0.0867, 0.0925	0.1676, 0.1916	0.1311, 0.1618

^{a} $R_1=\Sigma||F_o|-|F_c||/\Sigma|F_o|$. ^{b} $wR_2=\{\Sigma[w(F_o{}^2 - F_c{}^2)^2]/\Sigma(F_o{}^2)^2\}^{1/2}$.

Table 2. Selected Bond Lengths (Å) and Angles (deg) for **1**−**4**

1		2		3		4	
Zn1−O3	2.097(3)	Cd1−O1*w*	2.265(3)	Zn1−O1*w*	2.096(3)	Zn1−O1*w*	2.152(3)
Zn1−O4	2.104(2)	Cd1−O3*w*	2.282(3)	Zn1−O2*w*	2.108(3)	Zn1−O2*w*	2.096(3)
Zn1−N3	2.115(3)	Cd1−O2*w*	2.301(3)	Zn1−O3*w*	2.144(3)	Zn1−O3*w*	2.102(2)
Zn1−O6	2.115(3)	Cd1−N4	2.341(3)	Zn1−O4*w*	2.115(3)	Zn1−O4*w*	2.104(3)
Zn1−O5	2.158(2)	Cd1−N2	2.360(3)	Zn1−N1	2.177(3)	Zn1−N1	2.163(3)
Zn1−N1	2.168(3)	Cd1−N1	2.367(3)	Zn1−N3	2.116(3)	Zn1−N3	2.119(3)
O3−Zn1−O4	92.5(1)	O1*w*−Cd1−O3*w*	175.6(1)	O1*w*−Zn1−O2*w*	93.8(1)	O2*w*−Zn1−O3*w*	92.5(1)
O3−Zn1−N3	89.2(1)	O1*w*−Cd1−O2*w*	85.5(1)	O1*w*−Zn1−O4*w*	177.9(1)	O2*w*−Zn1−O4*w*	177.4(1)
O4−Zn1−N3	92.8(1)	O3*w*−Cd1−O2*w*	91.0(1)	O2*w*−Zn1−O4*w*	85.1(1)	O3*w*−Zn1−O4*w*	85.4(1)
O3−Zn1−O6	177.6(1)	O1*w*−Cd1−N4	93.4(1)	O1*w*−Zn1−N3	88.9(1)	O2*w*−Zn1−N3	89.0(1)
O4−Zn1−O6	85.6(1)	O3*w*−Cd1−N4	90.4(1)	O2*w*−Zn1−N3	91.6(1)	O3*w*−Zn1−N3	92.8(1)
N3−Zn1−O6	92.4(1)	O2*w*−Cd1−N4	174.0(1)	O4*w*−Zn1−N3	92.9(1)	O4*w*−Zn1−N3	92.7(1)
O3−Zn1−O5	87.0(1)	O1*w*−Cd1−N2	89.4(1)	O1*w*−Zn1−O3*w*	87.1(1)	O2*w*−Zn1−O1*w*	87.3(1)
O4−Zn1−O5	83.8(9)	O3*w*−Cd1−N2	88.3(1)	O2*w*−Zn1−O3*w*	84.4(1)	O3*w*−Zn1−O1*w*	83.6(1)
N3−Zn1−O5	174.9(1)	O2*w*−Cd1−N2	96.0(1)	O4*w*−Zn1−O3*w*	91.0(1)	O4*w*−Zn1−O1*w*	90.8(1)
O6−Zn1−O5	91.3(1)	O3*w*−Cd1−N1	86.6(1)	N3−Zn1−O3*w*	174.1(1)	N3−Zn1−O1*w*	174.8(1)
O3−Zn1−N1	91.6(1)	O2*w*−Cd1−N1	89.0(1)	O1*w*−Zn1−N1	92.0(1)	O2*w*-Zn1−N1	91.8(1)
O4−Zn1−N1	171.6(1)	N4−Cd1−N1	85.7(1)	O2*w*−Zn1−N1	171.5(1)	N3−Zn1−N1	94.6(1)
N3−Zn1−N1	94.6(1)	N2−Cd1−N1	173.2(1)	O4*w*−Zn1−N1	88.9(1)	O4*w*−Zn1−N1	90.1(1)
O6−Zn1−N1	90.1(1)	N4−Cd1−N2	89.9(1)	N3−Zn1−N1	94.7(1)	O1*w*−Zn1−N1	89.3(1)
O5−Zn1−N1	89.0(1)	O1*w*−Cd1−N1	96.0(1)	O3*w*−Zn1−N1	89.7(1)	O3*w*−Zn1−N1	171.5(1)

$C_{64}H_{76}Zn_2N_{12}O_{24}Cl_2$ (%): C, 48.07; H, 4.79; N, 10.51. Found: C, 48.11; H, 4.75; N, 10.61. IR frequencies (KBr, cm^{-1}): 3374, 1628, 1596, 1542, 1488, 1425, 1365, 1330, 1201, 1166, 1098, 1059, 1006, 813, 702.

Crystal Structure Determination. Single crystal X-ray diffraction data collections of **1**–**4** were performed on a Bruker Apex II CCD diffractometer operating at 50 kV and 30 mA using Mo Kα radiation (λ = 0.71073 Å). Data collection and reduction were performed using the APEX II software.[19] Multiscan absorption corrections were applied for all the data sets using the APEX II program.[19] All four structures were solved by direct methods and refined by full-matrix least-squares on F^2 using the SHELXTL program package.[19] All nonhydrogen atoms were refined with anisotropic displacement parameters. Hydrogen atoms attached to carbon were placed in geometrically idealized positions and refined using a riding model. Hydrogen atoms on water molecules or amino groups were located from difference Fourier maps and were also refined using a riding model. Crystallographic data for **1**−**4** are listed in Table 1 and selected bond lengths and angles for all compounds are given in Table 2. More details on the crystallographic information, as well as refinement data, and anisotropic displacement parameters can be found in the Supporting Information.

Results and Discussion

Structures. Single crystal X-Ray analysis revealed that compounds **1** and **2** have the same ligand components but different structural topologies. The asymmetric unit of **1** contains $[Zn(bipy)_{1.5}(H_2O)_4]^{2+}$, one isolated bipy ligand, two water molecules, one deprotonated paba ligand, and one disordered ClO_4^- anion (Figure 1). The Zn center is six-coordinated by four aqua ligands and two nitrogen atoms from two different bipy ligands. Interestingly, only one bipy molecule acts as a bidentate bridging ligand between two zinc metal ions while the other two function only as monodentate terminal ligands. This results in the formation of a (3 + 2) "Z" host unit (Figure 2a and corresponding schematic mode Figure 2d), which in turn is infinitely extended via face to face $\pi\cdots\pi$ interactions among the pyridine rings of the bipy ligands to form zigzag chains

---

(19) (a) Bruker AXS Inc. *APEXII software*, Version 6.12; Bruker AXS Inc.: Madison, Wisconsin, U.S.A., 2004. (b) Sheldrick, G. M. *SHELXL-97, Program for X-ray Crystal Structure Refinement*; University of Göttingen: Göttingen, Germany, 1997.

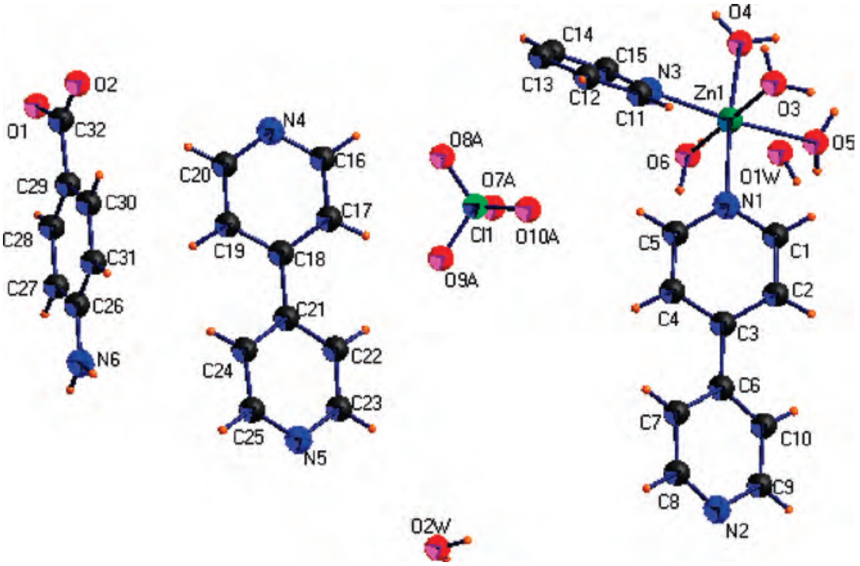

Figure 1. Perspective view of the asymmetric unit of **1** (disorder of the perchlorate anion is omitted for clarity).

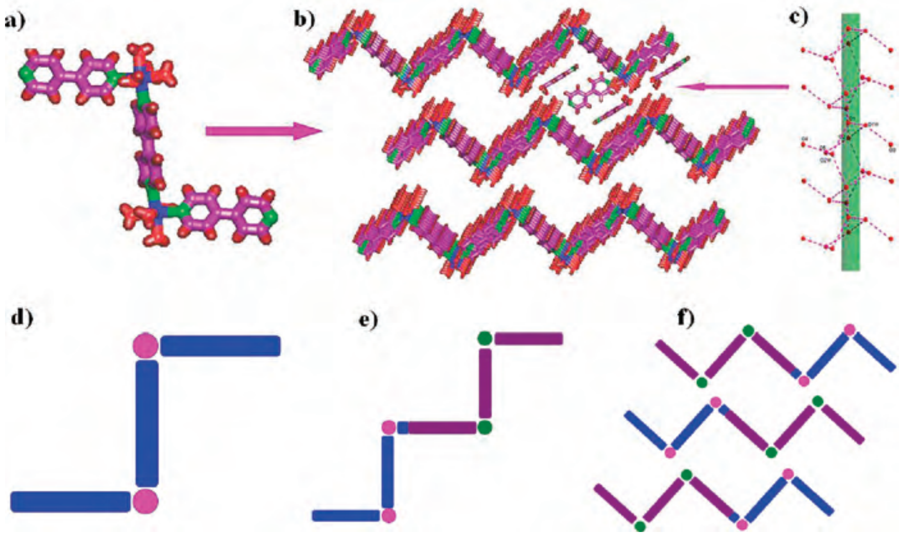

Figure 2. View of the “Z” host unit of **1** (a) and the corresponding schematic mode (d); the $\pi\cdots\pi$ contacts of two adjacent 4,4′-bipy ligands of the “Z” host units form infinite zigzag chains (b), and the corresponding schematic mode is depicted in (e); (c) the chain of hydrogen bonded water molecules forming the flexible joint between the zigzag chains.

that in turn are stacked atop of each other along the [010] direction to form infinite zigzag layers as shown in Figure 2b. The corners of these layers, made up by the $Zn(OH_2)_4$ groups, are surrounded by the solvate water molecules and the carboxylate oxygen atoms of the paba ions, and all of these are connected to each other via strong $O-H\cdots O$ hydrogen bonding interactions (see Supporting Information Table 1). Through these hydrogen bonds the zigzag layers are connected with each other via the $Zn(OH_2)_4$ corners to form a 3D grid network with a large cavity that stretches infinitely parallel to the *b*-axis (Figure 2b and the corresponding schematic mode in Figure 2f). The representation differs from that reported in the literature in which 4,4′-bipy ligands bridge metal ions to construct 2D or 3D grid networks.[10–13] The conglomerate of water molecules around the $Zn(OH_2)_4$ units, which might be best described as a flexible joint between the individual zigzag chains and layers, forms an infinite water cluster chain parallel to the *b*-axis (Figure 2c). The dimensions of the large cavities that stretch through the whole crystal are approximately 17.0 × 13.0 Å^2. The (4 + 6) grid cavity is occupied by the not-metal-coordinated bipy and paba molecules and the perchlorate anions. Both the bipy as well as the paba molecules are both hydrogen bonded to the water molecules in the above-mentioned cluster chains. The isolated pyridine rings of the bipy ligand are noncoplanar with a dihedral angle of 19.94°. Despite this tilt angle, these bipy molecules are also forming infinite stacks via $\pi-\pi$ interactions with centroid to centroid distances of 3.626(3) and 3.719(4) Å, respectively. They are also involved in $C-H\cdots\pi$ interactions with the aromatic rings of neighboring paba ligands. The size of the void encapsulated by the network (bipy, paba, ClO_4^-, and water solvent) is 2145.2 Å^3, which is 59.6% of the total volume as estimated using the Platon software.[18]

---

(20) Supporting information on spectral data is available.

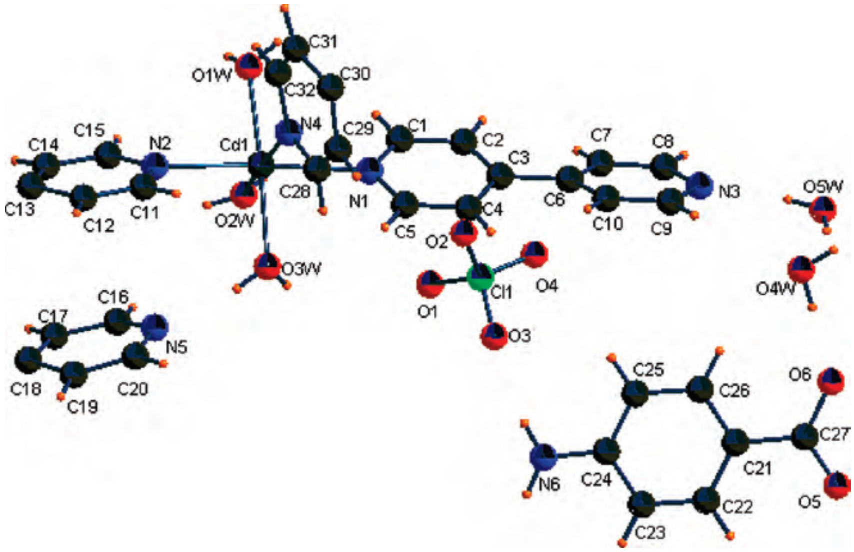

Figure 3. Perspective view of the asymmetric unit of **2** (disordered sections are omitted for clarity).

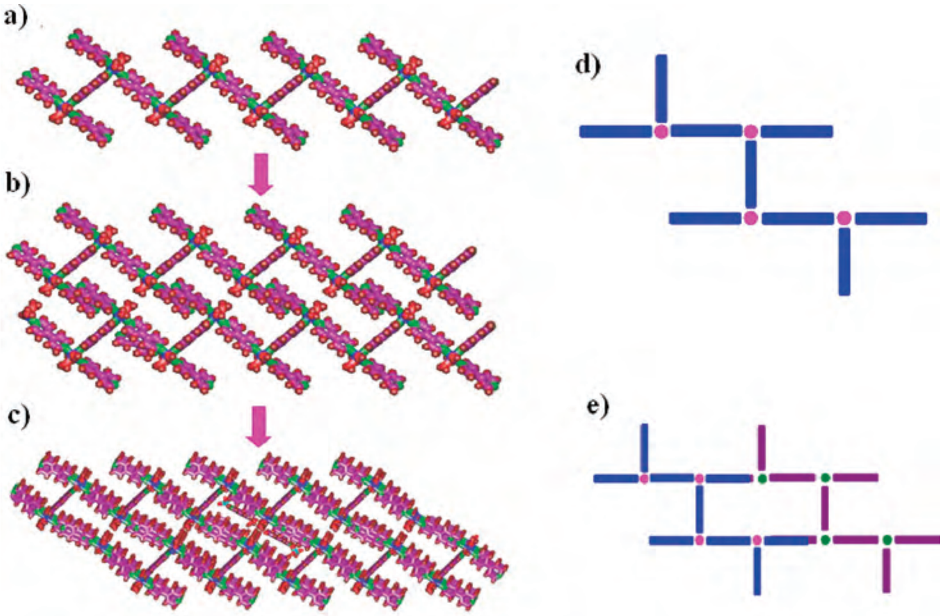

Figure 4. View of the unprecedented alternately inverse "T" chain of **2** formed via 4,4′-bipy connecting the metal ions (a) and the corresponding schematic mode (d); the $\pi\cdots\pi$ overlap of two adjacent 4,4′-bipy ligands of the chains form an extended porous layer (b) and the corresponding schematic mode (e).

The asymmetric unit of **2** contains one $[Cd(bipy)_2(H_2O)_3]^{2+}$ cation, half a bipy ligand, two and one-half water molecules, one deprotonated paba ligand, and one ClO_4^- anion (Figure 3). The compound shows a systematic 1:1 disorder of large parts of the structure.[20] This disorder originates from an alternating presence of either two or three interstitial water molecules between neighboring paba ligands. The carboxylate O atoms of the paba ions and these water molecules are arranged in a chain along the *a*-axis, and the alternation of the number of water molecules then causes a 1:1 disorder of the paba ligands along these chains of the type pabaA$\cdots$3$H_2O$$\cdots$pabaB$\cdots$2$H_2O$$\cdots$pabaA$\cdots$3$H_2O$$\cdots$pabaB$\cdots$2$H_2O$$\cdots$ in which the carboxylate unit of the paba ions is pushed either toward or away from the interstitial water molecules (orientation pabaA and pabaB, Supporting Information Figure 2S_2).[20] Additional 1:1 disorder is observed for some of the 4,4′-bipy molecules (Supporting Information Figure 2S_3).[20] Both types of disorder, while extensive, are systematic, largely limited to the solvate and encapsulated molecules, and do not affect the overall molecular framework observed for compound **2**.

The Cd ion in **2** is coordinated by three nitrogen atoms from three different bipy ligands; the other three sites on the metal ion are occupied by aqua ligands. Two of the bipy molecules, in the cis-position to each other, act as bidentate bridging ligands; the third, trans to the first and cis to the second, is a monodentate terminal ligand. As a result, an alternately inverse "T" chain is formed (Figure 4a and the corresponding schematic mode in Figure 4d). A careful review of the literature[10–13] suggests that the fashion in which these 4,4′-bipy molecules coordinate to the metal ions is unprecedented. The individual chains are stacked atop of each other along the *a*-axis, and the terminal 4,4′-bipy ligands are linked via $\pi\cdots\pi$ interactions to their counterparts in neighboring chains to give a (6 + 6) 3D grid with the dimensions of approximately 25.5 × 8.5 Å^2 (Figure 4b and the corresponding schematic mode in Figure 4e). The thus created infinite channels along the *a*-axis are filled with the paba and perchlorate ions, and the interstitial water molecules and the 4,4′-bipy molecules are not directly coordinated to the Cd atom and make up about 51.1% of the total volume of the crystal structure. The isolated 4,4′-bipy ligands are connected to the Cd(OH$_2$)$_2$ unit via O−H···N hydrogen bonds and are forming $\pi\cdots\pi$ stacks with neighboring Cd-coordinated 4,4′-bipy ligands (Figure 4c). A pair of centrosymmetrically orientated paba and ClO_4^- anions are accommodated in the cavity via hydrogen bonding interactions. The carboxyl oxygen atoms, coordinated water molecules, and the uncoordinated water molecules located in the cavity also form an oxygen cluster network via hydrogen bonding contacts that is similar to the one formed in compound **1**.[20]

Properties. As the anions and interstitial water molecules that occupy the large voids are only held in place via (relatively) weak hydrogen bonding interactions, we wanted to test if they might show a high enough mobility to allow their exchange without destruction of the framework. To investigate the ion-exchange properties of these materials, the excellent single crystals of **1** were immersed in an aqueous NH_4PF_6 solution (0.2 mmol) over one week and then its structure was remeasured under identical conditions, yielding a single crystal X-ray data set for the hexafluoro phosphate compound **3** of similar quality as the original one for **1**. The perchlorate anions were 100% replaced by the slightly larger hexafluorophosphate anions, giving rise to an increase in the unit cell size by 113.6 Å^3 for **3** (see Supporting Information Figure 3S).[20] The molecular framework is basically unchanged when compared with **1**, and the average Zn−O/N distances are almost identical. When the crystals of **3** were immersed in an aqueous $NaClO_4$ solution (0.2 mmol), structure **4** (viz. **1**) was reestablished (Supporting Information Figure 4S),[20] demonstrating a completely reversible ion exchange between ClO_4^- and PF_6^-. This transformation can be significantly accelerated by removal of the noncoordinated water molecules prior to reimmersion in an aqueous solution of the other anion. A crystalline sample of **1** when heated in the solid state to 60 °C for 3 h loses the noncoordinated water molecules (see Supporting Information Figure 5S with thermogravimetric analysis (TGA) results).[20] The resulting solid sample was immersed in an aqueous NH_4PF_6 solution for 30 min, and then filtered off and dried after thoroughly washing with water. The IR spectrum of this sample also shows the disappearance of an intense ClO_4^- peak (1165–1097 cm^{-1}) and the appearance of equally intense PF_6^- peaks (850 and 569 cm^{-1}) indicating that the sample has undergone ion-exchange and vice vera.

To examine the potential of compound **1** for the sensing of different anions, its fluorescence properties in an ethanol/water (1:1, v/v) solution were studied. The solution of compound **1** exhibits intense photoluminescence upon excitation at 320 nm. The 4,4′-bipy alone exhibits no photoluminescence, and the paba acid shows a 347 nm emission band. Therefore, the emissions of **1** (λ_{max} = 347 and 467 nm) may be attributed to the emission of the free paba (λ_{max} = 347 nm) and the ligand-to-metal charge transfer (LMCT)[21] (λ_{max} = 467nm, Supporting Information Figure 7S). A standard aqueous solution of sodium salts of Br$^-$, NO_3^-, and IO_4^- and ammonium salts of BF_4^- and PF_6^- were added stepwise to the sample solution of **1** (0.3 mg/mL) at room temperature. As shown in Figure 5, when a standard solution of NH_4PF_6 was added to a solution of **1**, the bands at 347 and 467 nm increased with the addition of the hexafluorophosphate, followed by a stepwise decrease, thus indicating a continuous reduction of the solution concentration after reaching at 1:1 stoichiometry for ClO_4^- and PF_6^- ($\mathbf{1} + PF_6^- \rightleftharpoons \mathbf{3} + ClO_4^-$). However, other aqueous solutions of sodium salts of Br$^-$, NO_3^-, and NO_2^- and ammonium salts of BF_4^- did not exhibit the same effect as observed for the PF_6^- anion (Supporting Information Figure 7S−9S). The intensity enhancement is not dependent on the cation as no signal increase was observed with aqueous solutions of NaBr and $NaNO_3$. Addition of aqueous solution of the aforementioned salts into solutions of the paba ligand also showed no large changes in the emission spectra. Therefore, we believe that because of its larger size the PF_6^- anion may interact more strongly with the other components of the structure, for example, through hydrogen bonding, than the ClO_4^- anion. The assumption that the larger size of the PF_6^- anion is causing the observed changes in the emission spectra is supported by the observations made for the even larger $NaIO_4$ anion. Upon stepwise addition of a standard $NaIO_4$ solution, the emission intensity at 344 nm of the paba ligand initially increases to almost two times its original state, followed by

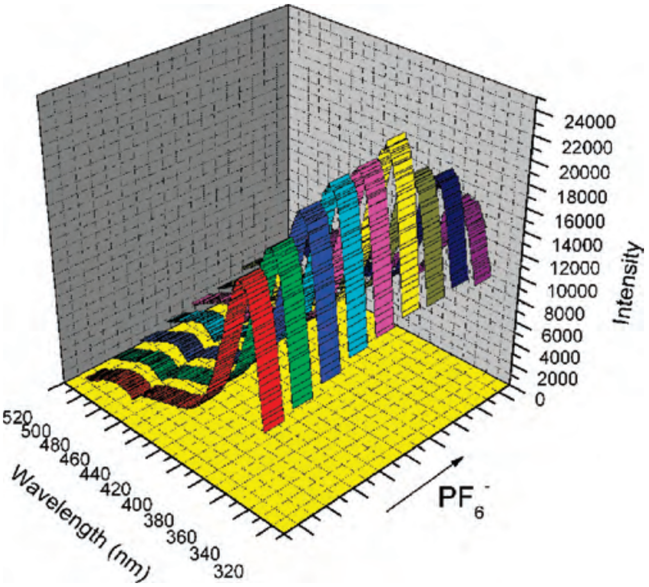

Figure 5. Fluorescence spectra of **1** followed by addition of the aqueous solution of NH_4PF_6.

---

[21] (a) Bertoncello, R.; Bettinelli, M.; Cassrin, M.; Gulino, A.; Tondello, E.; Vittadini, A. *Inorg. Chem.* **1992**, *31*, 1558. (b) Dai, J.-C.; Wu, X.-T.; Fu, Z.-Y.; Cui, C.-P.; Hu, S.-M.; Du, W.-X.; Wu, L.-M.; Zhang, H.-H.; Sun, R.-Q. *Inorg. Chem.* **2002**, *41*, 1391.

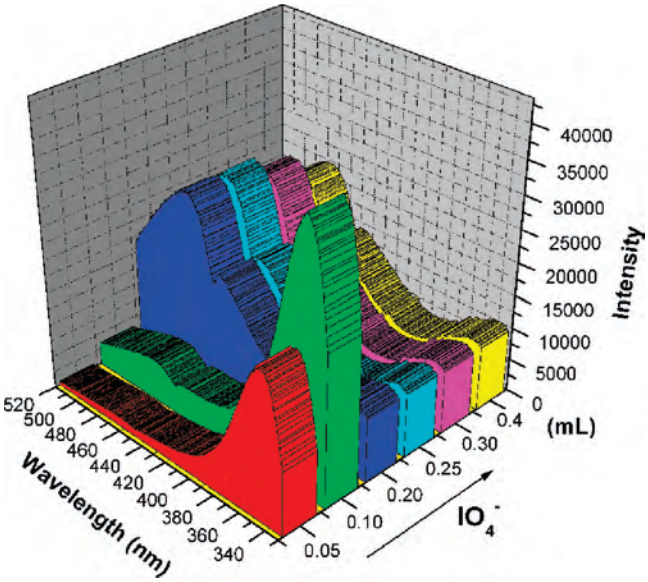

Figure 6. Fluorescence spectra of **1** followed by addition of the aqueous solution of $NaIO_4$.

nearly total quenching of this signal above the addition of 1 equiv of $NaIO_4$ (Supporting Information Figure 10S). Instead the LMCT emission band at 472 nm grows in Figure 6 and then slightly decreases upon addition of even more $NaIO_4$. We attribute these dramatic changes to the much larger size of the IO_4^- anion. Addition of IO_4^- seems to break the original solution state of the sample and possibly induces the free paba ligand to coordinate to the metal center in the new solution system (thus quenching the emission of the paba ligand and enhancing that of the LMCT). The IO_4^- ion, it seems, cannot be accommodated in the voids vacated by the smaller ions. Further study of the behaviors of these anions is underway and reported elsewhere.

Conclusions

In summary, two novel d^{10} metal organic frameworks with large voids were constructed with the help of 4,4′-bipy and paba ligands. The 4,4′-bipy ligands exhibit two new coordination modes to the metal ions. Compound **1** shows perfect reversible anion exchange to form the hexafluorophosphate derivative **3**, and, in solution, it exhibits attractive anion sensing properties. These results further highlight the complexities of the self-assembly process and the need to understand the relative importance of the interactions between metal ions, ligands, and solvents, as well as the anions, during the crystallization process.

Supporting Information Available: X-ray crystallographic information files (CIF) for compounds **1**, **2**, **3**, and **4**, hydrogen bonding tables, TGA traces, and additional figures. This material is available free of charge via the Internet at http://pubs.acs.org.

IC702366T